Angular Correlation of Annihilation Radiation in Alkali Halide Crystals*

W. E. MILLETT AND R. CASTILLO-BAHENA†
The University of Texas, Austin, Texas
(Received June 7, 1957)

A new type of instrument has been used for measurements on Mg metal and single crystals of LiF, NaCl, KCl, KBr, and KI. The data, after correction for instrument resolution, yield the momentum distribution of either the photons or the center of mass of the positron and electron just prior to annihilation. The momentum distribution obtained for NaCl is accounted for by assuming (a) that the positron is bound to the chloride ion in an s state, (b) that annihilation takes place with one of the electrons of the closed shell, and (c) that the overlap wave function is of the form $(r-b)^2e^{-mr}$. Best agreement with experiment was obtained for 30% of the annihilations taking place with s electrons for which $b=0.75$ A, and $m=3.64$ A^{-1} and the other 70% with p electrons for which $b=0.70$ A and $m=4.00$ A^{-1}.

I. INTRODUCTION

THE measurement of the angular correlation of two-photon annihilation radiation will, when the data are corrected and properly analyzed, lead to the distribution of the total momentum of the positron and electron just prior to annihilation.[1] The value of such information is strengthened considerably by theoretical calculations which indicate that a positron is reduced to thermal energies before it is annihilated.[2] The results obtained for positrons annihilating in certain metals confirm these calculations,[3] since the momentum distribution obtained is largely that expected on the basis of the Fermi distribution of the free electrons.

The alkali halides are of interest since they are ionic crystals. This provides the possibility of the positron becoming bound to the negative or halogen ion.[4] The binding energy of the positron to the isolated chlorine ion as calculated by Simons[5] is 3.74 ev in the ground state. When one takes into account the Madelung correction due to the neighboring ions in the crystal,[6] the binding energy in NaCl is 8.4 ev.[7]

Although the alkali halides have already been studied by Lang,[8] our results are reported here since we have obtained more detail. Since the experimental arrangement used in this investigation is basically different than that used in other measurements of this type, a detailed description of the apparatus is included here.

The measurements which have been reported thus far have in every case determined a set of numbers proportional to the probability that the total momentum of the annihilation photons has a z component lying between p_z and $p_z+\Delta p_z$. The probability that the total momentum of the annihilation photons, p, lies between p and $p+\Delta p$, i.e., $N(p)\Delta p$, is obtained from the data as follows. Let the coincidence counting rate measured at an angle θ, after correction for instrument resolution, be represented by $C_z(\theta)$. Then

$$N(p)\propto\theta dC_z(\theta)/d\theta,$$

where p is equal to θ times the momentum of an annihilation photon, i.e., $p=\theta mc$.[3]

The apparatus described here yields, after correction for instrument resolution, numbers which are proportional to the probability that the total momentum has a ρ component in cylindrical coordinates which lies between p_ρ and $p_\rho+\Delta p_\rho$, i.e., $C(p_\rho)\Delta p_\rho$. If we let $D(p_\rho)=C(p_\rho)/2\pi p_\rho$, then $D(p_\rho)\propto D(\theta)$, since $p_\rho=\theta mc$, and

$$N(p)\propto\theta_0^2\int_0^\infty\frac{1}{\theta_1}\frac{dD(\theta_1)}{d\theta_1}d\theta,$$

where $p=\theta_0 mc$ and $\theta_1=[\theta_0^2+\theta^2]^{\frac{1}{2}}$.

One advantage of the latter method is that $N(p)$ is determined with less error since it is obtained from a sum of slopes rather than from the slope at a point. As will be seen later, an additional advantage lies in the improved counting efficiency.

II. APPARATUS

1. Geometry

The experimental measurements determine the relative number of pairs of annihilation gamma rays having an angle between them which lies between $\pi-(\theta+\Delta\theta)$ and $\pi-\theta$. This relative number is determined by scintillation counters connected in coincidence as indicated in Fig. 1.

One of the collimators placed in front of the scintillation counters defines a narrow cone originating at the sample (collimator B, Fig. 2) while the other defines a

* Supported in part by the U. S. Air Force through the Air Force Office of Scientific Research of the Air Research and Development Command.

† Recipient of an E. D. Farmer Scholarship and a special study grant from the Instituto Technologico de Monterrey.

[1] Two recent review articles, S. Berko and F. L. Hereford, Revs. Modern Phys. **28**, 299 (1956) and R. A. Ferrell, Revs. Modern Phys. **28**, 308 (1956), contain background and references.

[2] R. L. Garwin, Phys. Rev. **91**, 1571 (1953); G. E. Lee-Whiting, Phys. Rev. **97**, 1557 (1955).

[3] A. T. Stewart, Can. J. Phys. **35**, 168 (1957).

[4] J. A. Wheeler, Ann. N. Y. Acad. Sci. **48**, 219 (1946).

[5] L. Simons, Phys. Rev. **90**, 165 (1953).

[6] N. F. Mott and R. W. Gurney, *Electronic Processes in Ionic Crystals* (Clarendon Press, Oxford, 1940), p. 71.

[7] Ferrell, in reference 1, p. 312, considers the Madelung correction to give rise to a decrease in binding energy and thus arrives at a negligible positron affinity.

[8] L. G. Lang, thesis, Department of Physics, Carnegie Institute of Technology, September, 1956 (unpublished).

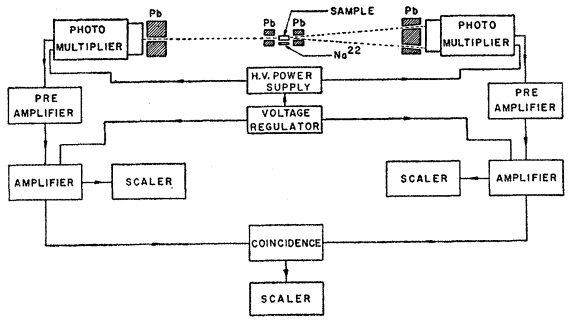

FIG. 1. Schematic diagram of apparatus.

thin conical shell coaxial with the cone defined by the first. This arrangement will admit in one direction gamma rays falling into a cone with a half-angle of one milliradian and in the opposite direction those falling into the conical shell with a half-angle Ω_2 and a thickness of plus and minus one milliradian. The coincidence circuit indicated that their time of arrival was in agreement to within 0.7 μsec.

The geometry is indicated schematically in Fig. 2. The distance L from the sample to collimator "A" was varied according to the angle Ω_2 to be selected and the particular collimators used. The range used was from one to two meters. The thickness of the conical shell was kept at 2 milliradians for Ω_2 set at an integral number of milliradians. The half-integral positions were obtained by keeping the collimator fixed and changing L appropriately. For convenience collimator "A" and its counter were set up on the carriage of a lathe with the axis parallel to the lathe bed. The source and sample holder was clamped to the head stock. The three sets of collimators were aligned with the aid of a surveyor's transit.

A source strength of approximately 0.7 millicurie gave a counting rate of about 1.3 counts/minute between 2 and 6 milliradians. We did not continue taking data when the counting rate dropped below 0.25 count/min. Approximately one month of continuous operation was required to take the data for each sample measured. The apparatus was checked frequently for reliability and reproducibility. The coincidence counting rate at a given angle Ω_2 was divided by the singles counting rate in "A" with the same collimator. Since the latter is proportional to the solid angle of collimator "A," this ratio is proportional to the coincidence counting rate per unit solid angle.

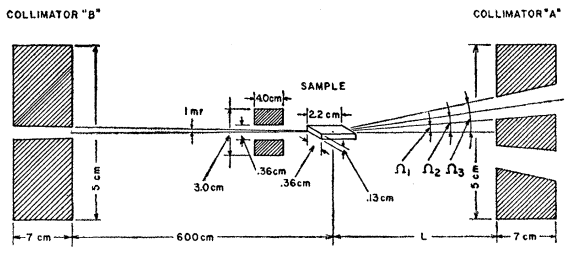

FIG. 2. Diagram of collimators and sample.

2. Calculation of Resolution

Before the data may be analyzed to determine the momentum distribution, they must be corrected for the finite resolution of the apparatus. To do this we must first calculate the resolution of the apparatus. This calculation must be carried out for each angle at which data were taken.

For a given collimator defined by the central angle Ω_2, we want to determine the relative probability of counting gamma rays correlated at some angle ψ. The first step in determining this probability is illustrated by Fig. 3. A point ρ_1,θ_1 in the sample is considered as the source of two gamma rays correlated at the angle ψ. If one of these gamma rays strikes collimator "B" at the point ρ,θ then the other gamma ray will strike collimator "A" somewhere on the approximately circular

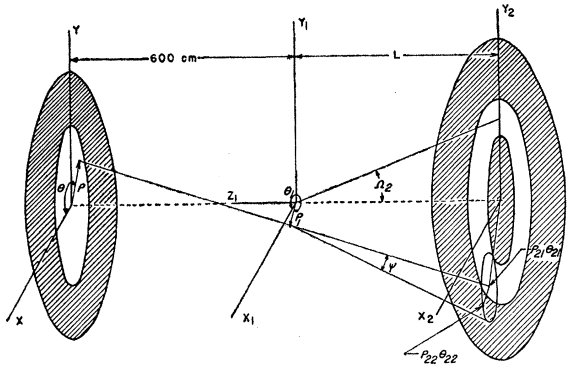

FIG. 3. Diagram illustrating the method of determining, for a given set of collimators defining the central angle Ω_2, the relative probability of counting gamma rays correlated at an angle ψ.

line indicated. The probability of this giving rise to a count is proportional to the length of arc falling within the opening in the collimator. This arc length is recorded for a fixed point in the sample (ρ_1,θ_1), while the point in collimator "B", (ρ,θ), is varied until the opening in collimator "B" is covered. Then a new point in the sample is used and the process is repeated. When the calculations have been carried out for all points in the sample the calculation is complete for that value of ψ. Now the calculation is repeated for other values of ψ until the resolution curve for Ω_2 is determined. The same calculation is carried out for all values of Ω_2. Three of the resolution curves obtained are shown in Fig. 4.

3. Data Correction

When all of the resolution curves are obtained, the data correction may be carried out. The procedure is one of trial and error.

To explain this procedure, let us assume that we guess the corrected data to be $T(\theta)$ and the resolution

curve for the collimator at the angle θ_n is given by $\Omega_n(\theta)$. Then let the generated function be defined by

$$G(\theta_n)=\int_0^\infty T(\theta)\Omega_n(\theta)d\theta.$$

When a $T(\theta)$ is found such that $G(\theta_n)$ equals the data measured at the angle θ_n and this equality holds for all values of θ_n for which data were taken, the $T(\theta)$ is the corrected data and it will be designated by $D(\theta)$. The trial function T is adjusted until this condition is satisfied.

The raw and corrected data for LiF are given in Fig. 5.

4. Momentum Distribution from the Data

Consider the meaning of the corrected coincidence rate per unit solid angle, i.e., $D(\theta)$. First note that by

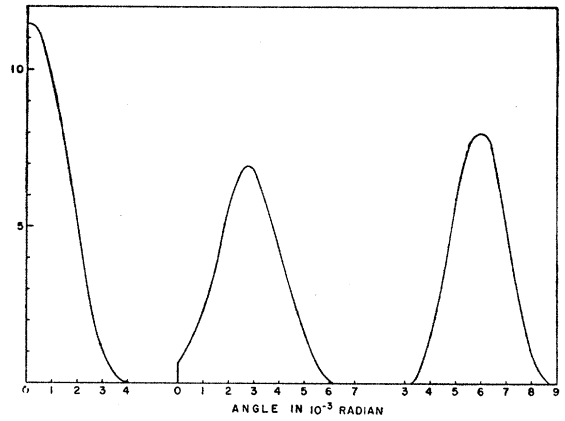

FIG. 4. Resolution curves obtained for the collimators defining the central angle Ω_2 equal to 1, 3, and 6 milliradians.

conservation of momentum the sum of the momentum of the positron and electron just prior to annihilation is equal to the sum of the momentum of the two annihilation gamma rays. The momentum sum, p, is very small compared to the momentum of one of the gamma rays which is approximately the rest mass of the electron times the speed of light, mc. The projection of the momentum sum onto a plane perpendicular to the direction of one of the gamma rays, $p_\perp$, is approximately θmc. The coincidence counting rate at a given angle θ is proportional to the probability that the momentum vectors in momentum space terminate on a thin cylindrical shell of radius $p_\perp=\theta mc$. The coincidence counting rate per unit solid angle is proportional to the probability that p falls in one narrow element of this cylindrical shell.

Now consider how these corrected data lead to the momentum distribution. Let $C(p_\rho)\Delta p_\rho$ be the probability that the vector $\mathbf{p}$ in momentum space will terminate somewhere on a cylinder of radius p_ρ and let $R(p)$

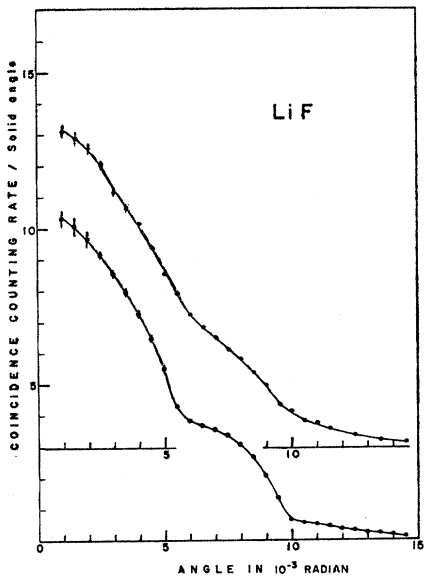

FIG. 5. Curves illustrating the effect of the correction for the instrument resolution. The upper curve gives the uncorrected data; the lower curve gives the data after correction. The uncertainties indicated are estimated probable errors.

be the density in momentum space such that

$$C(p_\rho)\Delta p_\rho=4\pi p_\rho\left\{\int_0^\infty R[(p_\rho^2+p_z^2)^{\frac{1}{2}}]dp_z\right\}\Delta p_\rho.$$

Note that the corrected coincidence counting rate at a given angle θ is proportional to $C(p_\rho)$, where $p_\rho=\theta mc$ and $C(p_\rho)/2\pi p_\rho\equiv D(p_\rho)$ is proportional to the corrected coincidence counting rate per unit solid angle. Then, by expressing $C(p_\rho)$ in terms of $D(p_\rho)$, we have

$$D(p_\rho)=2\int_0^\infty R[(p_\rho^2+p_z^2)^{\frac{1}{2}}]dp_z.$$

Now taking the derivative of both sides of this expression with respect to p_ρ,

$$\frac{dD(p_\rho)}{dp_\rho}=2\int_0^\infty\frac{\partial R[(p_\rho^2+p_z^2)^{\frac{1}{2}}]}{\partial p_\rho}dp_z.$$

The integral may be rewritten in terms of a derivative of R with respect to p:

$$\frac{dD(p_\rho)}{dp_\rho}=D'(p_\rho)=2\int_0^\infty\frac{dR}{dp}\frac{dp}{dp_\rho}dp_z.$$

Since

$$p^2=p_\rho^2+p_z^2 \quad\text{and}\quad dp=(p_\rho/p)dp_\rho,$$

it follows that

$$D'(p_\rho)=2p_\rho\int_0^\infty\frac{dR}{dp}\frac{1}{(p_\rho^2+p_z^2)^{\frac{1}{2}}}dp_z.$$

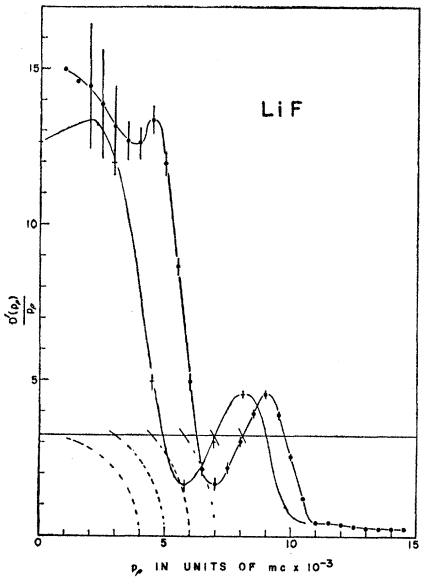

FIG. 6. Plot of $D'(p_\rho)/p_\rho$ *versus* p_ρ (the curve on the right). The uncertainties indicated are estimated probable errors. To replot this quantity *versus* $p_x=(p_\rho^2-p_y^2)^{\frac{1}{2}}$ for a particular p_y, each point is shifted to the left by the appropriate amount. This method is illustrated for the case $p_y=4mc\times10^{-3}$ by the curve on the left (for which the abscissa should now be read as p_x). The dashed circles indicate the geometrical construction of p_x from p_ρ for this value of p_y.

Now writing p_ρ as $(p_x^2+p_y^2)^{\frac{1}{2}}$, dividing both sides by p_ρ, and then integrating over p_x, we have

$$\frac{D'[(p_x^2+p_y^2)^{\frac{1}{2}}]}{(p_x^2+p_y^2)^{\frac{1}{2}}}dp_x = \int_0^\infty\int_0^\infty 2\frac{dR[(p_x^2+p_y^2+p_z^2)^{\frac{1}{2}}]}{dp}\frac{dp_z dp_x}{(p_x^2+p_y^2+p_z^2)^{\frac{1}{2}}}.$$

The double integral on the right may be expressed as a single integration by going to cylindrical coordinates, i.e., the double integral is replaced by

$$\pi\int_0^\infty \frac{dR}{dp}\frac{p_\rho dp_\rho}{(p_\rho^2+p_y^2)^{\frac{1}{2}}}=\pi\int_{p_y}^\infty\frac{dR}{dp}dp=-\pi R(p_y).$$

The probability that the total momentum lies between p and $p+\Delta p$, namely $N(p)\Delta p$, is found from the density $R(p)$ by the following relation:

$$N(p)\Delta p=4\pi p^2R(p)\Delta p.$$

Therefore, the probability $N(p)$ is obtained from the data by the following prescription:

$$N(p)=-4p^2\int_0^\infty\frac{D'[(p_x^2+p_y^2)^{\frac{1}{2}}]}{(p_x^2+p_y^2)^{\frac{1}{2}}}dp_x.$$

The fact that the data are taken for a particular p_ρ and $D'(p_\rho)/p_\rho$ is integrated over p_x is only a minor inconvenience since the abscissa is just transformed by the relation $p_\rho^2=p_x^2+p_y^2$. The derivative of the corrected data is obtained by a least squares method. The integration is obtained with the aid of a planimeter.

A plot of $D'(p_\rho)/p_\rho$ *versus* p_ρ for LiF is given in Fig. 6. The abscissa transformation is illustrated for $p_y=4mc\times10^{-3}$.

III. RESULTS

1. Check on Method

A check on the operation of the apparatus and the method of analyzing the data is obtained from the measurements on magnesium. When a high-speed positron enters a metal it is rapidly slowed down to thermal energies and is then annihilated by one of the conduction electrons. For metals the density function $R(p)$ equals unity up to the Fermi energy and then it abruptly drops to zero. The $N(p)$ should then be proportional to p^2 up to the maximum p allowed, p_F, where $p_F^2/2m$ equals the Fermi energy, and then it should drop to zero. Our results are compared with the calculated Fermi distribution in Fig. 7. Note that the parabolic shape fits at the lower momenta. The solid line representing the Fermi distribution is extended until its area is equal to the area under the shaded portion of the data. The peak momentum determined in this manner yields an energy of 6.96 electron volts. If the valence of magnesium is taken to be 2.00, the Fermi energy is calculated to be 7.09 ev. This represents an error of 1.8% in the energy. More extensive measurements and analysis are needed, however, to determine whether or not this agreement is fortuitous.

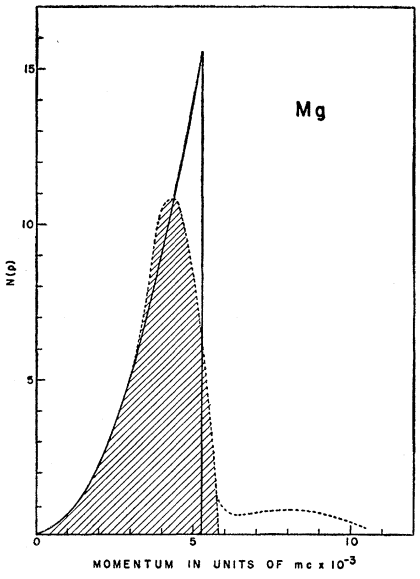

FIG. 7. Comparison of the experimental momentum distribution for magnesium, dashed curve, with the calculated Fermi distribution, solid curve. The area under the shaded portion of the dashed curve is the same as that under the solid curve.

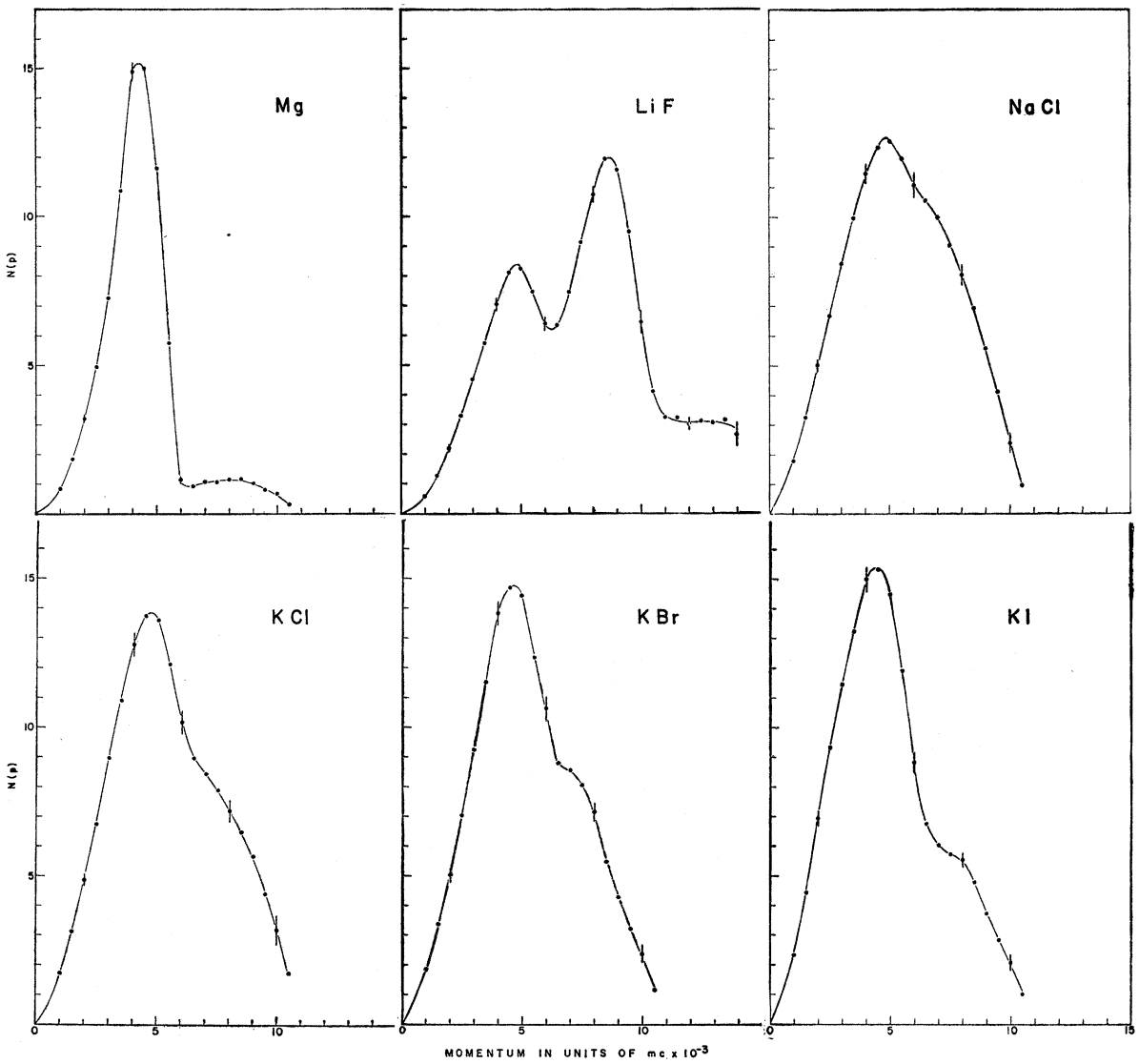

FIG. 8. The experimental momentum distributions obtained for Mg, LiF, NaCl, KCl, KBr, and KI. The estimated probable errors for some of the points are indicated.

2. Alkali Halide Crystals

The $N(p)$ *versus* p curves obtained for Mg, LiF, NaCl, KCl, KBr, and KI are given in Fig. 8. The estimated probable errors for some of the points are indicated.

To account for the shape of the $N(p)$ curves, we assume the positron is bound to the halogen ion and that annihilation takes place with one of the two s electrons or six p electrons in the closed shell of the halogen ion to which it is bound. The bound positron is assumed to be in an s state. The total momentum of the two annihilation gammas is assumed to be equal to the vector sum of the momentum of the positron and electron just prior to annihilation.

If we knew the wave functions of the positron and electron, the momentum distribution of the annihilation radiation could be determined. Ferrell[1] has indicated that

$$N(p) \propto k^2 \left[\int e^{-i\mathbf{k}\cdot\mathbf{r}} \psi\varphi d\tau \right]^2,$$

where $p=\hbar k$, $\psi\varphi$ is the product of the wave functions of the positron and electron, and $d\tau$ is the element of volume.

Ferrell[1] made an analysis of some $N(p_z)$ data for the alkali halides taken by Lang *et al.*[8] For this analysis he assumed the wave function of the positron to be a delta function. The momentum distribution obtained by such

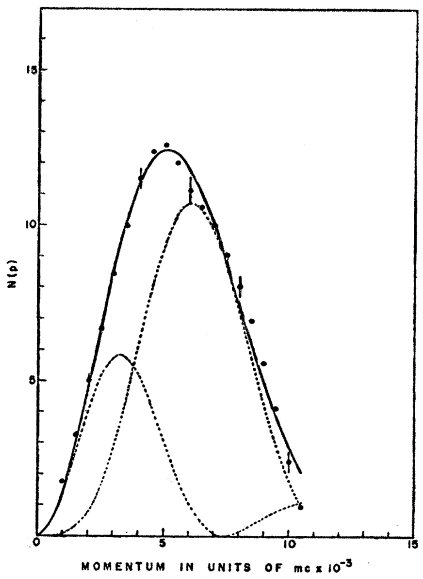

FIG. 9. Comparison of calculated and experimental momentum distributions obtained for NaCl. The individual contributions due to s and p electrons are indicated by the dashed curves, their sum by the solid curve, and the experimental values by the solid circles. The contribution due to s electrons is 30% of the total. The estimated probable errors for some of the points are indicated.

a wave function leads to a sequence of peaks which decrease only slightly in amplitude with increasing momentum.

In this analysis the product $\psi\varphi$ was taken to be

$$\psi_0\varphi_0=A_0(r-b_0)^2e^{-m_0r} \quad \text{for} \quad r>b_0$$
$$=0 \quad \text{for} \quad r<b_0,$$

for an s electron annihilating the s positron and

$$\psi_1\varphi_1=A_1(r-b_1)^2e^{-m_1r}\cos\theta \quad \text{for} \quad r>b_1$$
$$=0 \quad \text{for} \quad r<b_1,$$

for a p electron annihilating the s positron. The calculation was carried out for a wide range of parameters with the aid of a C.P.C. The fit was made for the momentum distribution obtained for NaCl. The parameters giving best fit for the annihilation with an s electron were $b_0=0.75$ A and $m_0=3.64$ A^{-1} and 29.8% annihilated in this way. For annihilation with a p electron $b_1=0.70$ A and $m_1=4.00$ A^{-1}. The results of this analysis are shown in Fig. 9. The dashed curves are the separate contributions for s and p electrons, the solid curve their sum and the solid circles the experimental values.

Further attempts are being made to account for the shape of the other $N(p)$ curves.

ACKNOWLEDGMENTS

We thank Dr. H. P. Hanson, Dr. H. Primakoff, and Dr. C. Herring for helpful and interesting discussions. We are grateful to Dr. L. G. Lang for pointing out an error in the data analysis. Ferrell's review[1] was of considerable aid in the interpretation of the NaCl data.